DEVELOPMENT OF AN ACTIVE FILM WITH NATURAL ZEOLITE AS ETHYLENE SCAVENGER

*A. COLOMA[1], F. J. RODRÍGUEZ [2,3], J. E. BRUNA [2,3], A. GUARDA [2,3], M. J. GALOTTO[2]**

1. Department of Agro-industries. Faculty of Agricultural Science. National University of the Altiplano, Puno, Perú
2. Center for the Development of Nanoscience and Nanotechnology (CEDENNA), Food Packaging Laboratory (LABEN-CHILE). Edificio Alimentos. Calle Obispo Umaña 050.Santiago. Chile
3. Food Science and Technology Department. Faculty of Technology. University of Santiago de Chile, Santiago, Chile. Avda Ecuador 3769. Santiago. Chile.

ABSTRACT

Ethylene (C_2H_4) acts as a plant hormone, growth regulator that has a number of effects on the growth. Ethylene accelerates respiration, leading to maturity and also softening and ripening of many kinds of fruits. Although ethylene has some positive effects, it is often hazardous to the quality and shelf-life of fruits and vegetables. The removal of ethylene and/or inhibition of the effect of ethylene in stored environments is fundamental to maintaining postharvest quality of climacteric produce. In this study, the efficiency of a Chilean natural zeolite (NZ-Ch) against a commercial Na^+ montmorillonite (Cloisite Na^+) was studied. The aluminosilicate characterization (XDR, FTIR, EGME, CEC, chemical composition) indicates that natural Chilean zeolite belongs to mordenite group. Elemental chemical analysis indicated that compensating ions, were sodium for $MTNa^+$ and calcium, sodium and potassium for NZ-Ch, and in both aluminosilicates copper was present in their composition. Ethylene adsorption kinetics were fitted to a pseudo-second order model. The rate constant of the ethylene adsorption was nearly double for NZ-Ch compared with $MtNa^+$. Langmuir-Freundlich isotherm allowed to determine maximum adsorption capacity that reached values of 5.4 µl g^{-1} for NZ-Ch and 1.28 µl g^{-1} for $MtNa^+$. Films of low density polyethylene (LDPE) were obtained with different NZ-Ch concentrations. After 50 hours, a removal of 37% of ethylene present on headspace was achieves with 10% of ZN-Ch in LDPE active films.

Keywords: Ethylene adsorption, Na^+ Montmorillonite, Natural Zeolite

INTRODUCTION

Ethylene (C_2H_4) is a naturally occurred, simple two carbon gaseous component that acts as a plant hormone, growth regulator that has a number of effects on the growth, development and storage periods of many kinds of fruits, vegetables and ornamental crops. Ethylene accelerates respiration, leading to maturity and also softening and ripening of many kinds of fruits. Moreover, ethylene accumulation can result in yellowing of green vegetables and it is responsible for numerous types of specific postharvest defects in fresh fruits and vegetables. Although ethylene has some positive effects, it is often hazardous to the quality and shelf-life of fruits and vegetables[1)]. Accumulation at trace levels of ethylene during the storage period may result in a number of specific defects and shorten the harvest shelf life[2)]. The removal of ethylene and/or inhibition of the effect of ethylene in stored environments is fundamental to maintaining postharvest quality of climacteric produce[3)]. In recent years, there has been a paucity of research on developing new and more efficacious ethylene scavenger materials. In contrast, there has been an exponential increase in research using the ethylene binding inhibitor 1-methylcyclopropene (1-MCP). Thus research activity has drifted away from ethylene removal to preventing the actions of ethylene through using 1-MCP.

Despite various ethylene scavenger technologies are available (e.g. high temperature catalytic degradation, activated carbon, etc.) most of the commercial ethylene control systems rely on both: adequate ventilation and oxidation of ethylene using potassium permanganate ($KMnO_4$)-based mechanisms. Ventilation, however, is not appropriate in sealed environments (controlled atmosphere) or where precise ethylene control is required[3)].

In the last decades, materials such as zeolites and clays (crystalline aluminosilicates) that possesses ethylene adsorption capacity, have received much attention[4,5)].

Clays and zeolites are aluminosilicates, which differ, in their crystalline structure. Clays have a layered crystalline structure and the zeolites have a rigid, 3-dimensional crystalline structure consisting of a network of interconnected tunnel and cage[6)]. Among clays, the montmorillonite is a natural layered clay, member of the smectite family. It is a 2:1 clay, meaning that it has two SiO_4 tetrahedral sheets sandwiching a AlO_6 central octahedral sheet. The presence of Al in the framework introduces negative charges that require the presence of charge balancing cations occupying interlaminar spaces[7)].

Zeolites are hydrated aluminosilicates of alkali and alkaline earth elements with unique crystal structures consisting of a three-dimensional framework of tetrahedral SiO_4 and AlO_4 in its framework structure[4)]. The isomorphic substitution of Si by Al, leads to a negative charge density in the zeolite lattice. This charge is neutralized by introducing monovalent, divalent or trivalent cations in the structural sites of the zeolite[8)]. Ion exchange of the balanced cations can result in clay and zeolites with specific properties such as selective adsorption. Erdogan et al. reported that natural zeolite (clinoptilolites) had considerable good ethylene removal properties[9)]. They found that zeolites containing K^+ ions showed greater capacity for ethylene adsorption than zeolite exchanged with Na^+ and Ca^{2+}. Sue-aok et al. reported the enhancement of ethylene adsorptivity upon modification of NaY zeolite by group I metal cations[8)]. Patdhanagul et al. demonstrated that zeolite NaY modified with phenyl trimethyl ammonium bromide (PTAB) as a cationic surfactant, is capable to modified only the external part of zeolite and not capable to enter the micropores of zeolite due to its large long chain, showing an appreciable increase in ethylene adsorption[2,4)].

On the other hand zeolite modified with palladium presented a significant ethylene adsorption capacity (4162 µLg^{-1} material), far superior to $KMnO_4$-based scavengers when used in low amounts (10 mg modified zeolite/L) and in conditions of high relative humidity[3)]. Modified zeolite was capable to increase kiwi and banana shelf-life although no effect was observed for strawberry.

The purpose of the current study is to compare the efficiency of a Chilean natural zeolite against Na^+ montmorillonite as ethylene scavenger, in order to select the best aluminosilicate to be modified to improve ethylene adsorption capacity, for the development of a new active packaging system.

EXPERIMENTAL PROCEDURE

Materials

Montmorillonite, Cloisite®Na^+ ($MtNa^+$), with a cationic exchange capacity (CEC) of 92.7 meq/100g was obtained from Southern Clay Products Inc. (Texas, USA). A Chilean natural zeolite (NZ-Ch) was supplied by Maderas Bravo S.A. (Talca, Chile). Lineal low-density polyethylene (LLDPE) and low density polyethylene (LDPE), were supplied by Dow Petroquímica S.A. (Chile).

Aluminosilicate characterization

Mineral moisture characterization

Moisture of the zeolite mineral was evaluated by gravimetric means. 1 g of each one of the aluminosilicates were dried at 100 ºC for 24 h in an oven (Binder, FD115, Tuttlingen, Germany), cooled in a desiccator and its mass was monitored in a precision balance (MS204, Mettler Toledo Greifensee,

e-mail: Maria.galotto@usach.cl

Switzerland) until constant weight (± 0.1 mg). The difference between the dried mass value and the equilibrium mass value was used to evaluate the moisture content[10].

Cation exchange capacity

Cation exchange capacity of the aluminosilicate was determined by chemical modification with NH_4^+ [10]. Aproximately 1 g of the aluminosilicate powder was mixed with 50 mL of $(NH_4)_2SO_4$ of a 0.25 mol L^{-1} and stirred for 16 h at room temperature. The final exchanged sample was centrifuged at 4000 rpm for 10 min, and washed with deionized water and dried overnight at 80 °C. Sample was then titrated with 0.1 mol L^{-1} NaOH standard solution. The cation exchange capacity was calculated from Equation 1.

$$CEC\ (meq\ g^{-1}) = \frac{(B-A)\times C}{m} \qquad [1]$$

where: CEC is meq g^{-1}; *B*: volume of NaOH used in the titration of blank (mL); A: volume of NaOH used in the titration of the sample (mL); C: concentration of NaOH (M); and *m*: weight sample (g).

Specific mass and specific surface area

The specific mass of the mineral was determined by pycnometry[11]. An amount of 10 g of aluminosilicate was inserted in a pycnometer with water at 25°C until fulfillment of the volume of the recipient and measured the different masses. Thus, using the known masses of water, sample and recipient, results obtained allowed to determine the specific mass of the mineral expressed in terms of gcm^{-3}. The specific gravity was calculated from equation 2.

$$Sg = \frac{W_2 - W_1}{(W_4 - W_1) - (W_3 - W_2)} \qquad [2]$$

The specific surface area (SSA) of the aluminosilicate was evaluated by ethylene glycol monometil ether (EGME) adsorption method. A sample of 0.5 g of aluminosilicate was dried at 110 ºC for 24 h. Approximately 3 mL of EGME was added to the material with a pipette and mixed together with a hand swirling motion to create uniform slurry. Afterward, samples were placed into a glass-sealed vacuum desiccator and allowed to equilibrate for 20 min. As a drying agent, a mix of 100 g 40-mesh anhydrous calcium chloride and 20 mL EGME desiccant was placed in a glass dish at the bottom of the desiccator. The desiccator was evacuated using a vacuum of 640 mm Hg. After the evacuation process, the samples were weighed every 10–12 h using an analytical balance (MS 204 Mettler Toledo, Greifensee, Switzerland). If the mass difference between the two measurements was more than 0.001 g, then the samples were placed into the desiccator again for additional vacuum. This process was continued until the sample weight did not change more than 0.001 g[12].

The quantity of EGME to cover 1 m^2 of material surface with a monomolecular layer is 2.86×10^{-4} g. The specific surface can be then calculated from the equation 3.

$$SSA_{EGME} = \frac{W_a}{0.000286\ W_s} \qquad [3]$$

where the SSA is in $m^2\ g^{-1}$; *Wa*=weight of EGME retained by the sample in grams; 0.000286=weight of EGME required to form a monomolecular layer on a square meter of surface (gm^{-2})[12]; and *Ws*=weight of soil in grams.

Particle size distribution

For the particle size analyses distribution of the minerals, 10 g sample was dispersed overnight in a mixture of 10 ml of sodium pyrophosphate solution at 5% w/v and 200 mL of double distilled water, keeping under stirring for 16 h. Thereafter, the sand size particles were separated from the suspensions by wet sieving through a 53-µm sieve. The fraction retained by the sieve was dried and then weighed. The clay fraction (< 2µm) was determined using the pipette method. The silt fraction (50µm-2mm) was determined by difference[12]. Analyses were performed in triplicates.

Chemical analysis

Samples (2g) were weighed and mixed with 20 mL HNO_3. After heating (100 °C) for 16 h, until complete evaporation of $HClO_4$, samples were left to cool at room temperature; 100 mL were gauged, filtered and measured in an inductively coupled plasma optical emission spectrophotometer (VARIAN Liberty RL Sequential ICP-OES, Mulgrave, Australia)[13].

X-ray diffraction (XRD)

XRD analysis was carried out in a Siemens Diffractometer D5000 (30 mA and 40kv) using CuKα (l=1.54Å) radiation at room temperature. All scans were performed in a 2q range 2–80º at 0.02º/seg.

Fourier transform infrared (FTIR)

This spectroscopic analysis was carried out in a Bruker IFS 66V spectrometer (Bruker Alpha, Ettlingen, Germany). The aluminosilicates were crushed and blended with KBr. Spectra were taken with 4 cm^{-1} resolution in a wave-number range from 4000–400 cm^{-1} with an average of 32 scans.

Ethylene adsorption

All ethylene adsorption experiments were carried out a room temperature (25ºC) in unstirred cell adsorption (Figure 1). Approximately 0.5 g of the sample, previously dried at 250 ºC for 24 h**,** was placed in a cell adsorption and sealed. Nitrogen:ethylene gas mixture (9.6 ppm v/v) were injected in the adsorption cell. Gas samples were extracted from the cell using a 5 mL syringe at 30 min intervals and analyzed in a gas chromatograph Perkin Elmer Clarus 500 (Shelton, USA) fitted with a flame ionization detector (FID) with a 0.53 mm I.D. and 50m length capillary column Rt™-Alumina PLOT. Oven and detector temperature were 100 °C and 250 °C respectively. Ethylene was calibrated against 9.6 µL L^{-1} ethylene balanced in N_2 (Linde Gas Chile S.A., Santiago, Chile). Helium gas was used as carrier at a flow of 10 mL / min.

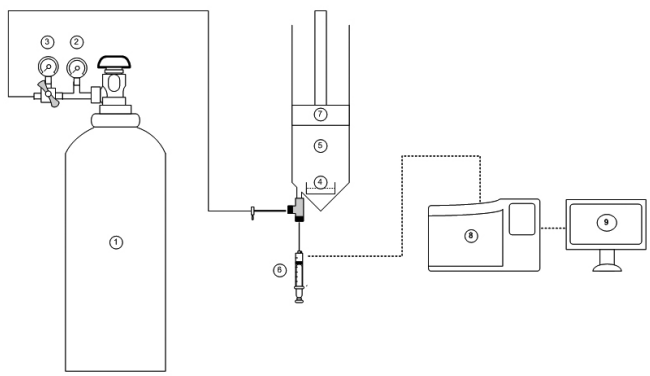

Figure 1: Schematic design of the volumetric adsorption system for aluminosilicates. (1) ethylene cylinder; (2) cylinder manometer; (3) mass flow meters; (4) sample; (5) adsorption cell; (6) sampling syringe; (7) Embolus; (8) gas chromatographic; (9) computer.

Adsorbed amount of ethylene (q_e), was expressed as removed volume per mass unit of adsorbent material (mL g^{-1}), and was calculated from the experimental data [C_i, C_f, V_L y *m*] in each sample according to the equation 4:

$$q_e = \frac{[C_i - C_f] \times V}{m} \qquad [4]$$

where *V* is the free volume of the cell adsorption (L), C_i is the initial concentration in the cell adsorption (µl L^{-1}), C_f is the final concentration in the cell adsorption (µl L^{-1}), m is the mass of adsorbent material (g).

Adsorption Kinetics model

Adsorption kinetics is one of the most important parameters for determining the adsorption mechanism and also to investigate the efficacy of adsorbent for removal of ethylene. In this study kinetic model pseudo-first order was used to predict the sorption behavior of the data[14,15].

$$\ln(q_e - q_t) = \ln q_e - k_1 t \qquad [5]$$

where q_e (µL g^{-1}) and q_t (µL g^{-1}) are the amount of ethylene adsorbed by aluminosilicate at equilibrium conditions, and at time (*t*), respectively. k_1 (h^{-1}) is the rate constant of pseudo-first-order kinetic model[16]. k_1 and q_e were determined from the slope and intercept of ln ($q_e - q_t$) versus *t*, respectively. The pseudo-second-order model was also fitted to the adsorption data using the following equation:

$$\frac{t}{q_t} = \frac{1}{k_2 q_e^2} + \frac{t}{q_e} \qquad [6]$$

Where k_2 (g µl^{-1}h^{-1}) is the constant of pseudo-second order.

Adsorption Isotherms model

The experimental adsorption isotherms of ethylene on material adsorbent were fitted to the Langmuir–Freundlich isotherm model, equation 7:

$$q^* = \frac{q_m b\, C_e^{\left(\frac{1}{n}\right)}}{1 + b\, C_e^{\left(\frac{1}{n}\right)}} \qquad [7]$$

where q^* is the adsorbed amount at equilibrium concentration C_e, q_m the saturated adsorbed amount, b and n are the isotherm parameters. 'b' represents the strength of the interaction between the adsorbate and the adsorbent, and 'n' can be regarded as the parameter characterizing the system heterogeneity[17].

Ethylene adsorption kinetic curves were fitted using the program OriginPro8.

Preparation of active films

In order to favor a good mixing between the LDPE and NZ, a 70:30 % w/w mixture of LDPE/NZ-Ch masterbatch was previously prepared. The compounding processes of masterbatch production was performed using a co-rotating twin-screw extruder LabTech Scientific LTE20 (Bangkok, Thailand) having a screw diameter of 20 mm and a barrel length of 800 mm (L/D = 40). The LDPE/NZ-Ch powdery mixture was fed into the hopper by gravimetric dosing. The mixed compounds extruded through a round die was immediately passed through a LabTech Scientific LW-100 (Bangkok, Thailand) cold-water bath, and then the solidified long strands of composite were pelletized in a LabTech Scientific LZ-120 (Bangkok, Thailand) at 8 rpm. The temperature profiles of extruder from Zone 1 to Zone 10 were kept between 115 and 130°C. The twin-screw speed and single screw hopper feeder were fixed at 40 rpm.

Masterbatch was diluted with LDPE pellets to prepare LDPE/NZ-Ch films with different content of NZ-Ch: 2.5, 5.0, 7.5 and 10.0 % w/w. Corresponding mixture of masterbatch and LDPE pellets was processed into a co-rotating twin-screw extruder LabTech Scientific LTE20 (Bangkok, Thailand) with a wide die (200 mm). The temperature profiles of extruder from Zone 1 to Zone 10 were kept between 170 and 185°C. The twin-screw speed was fixed at 80 rpm and single screw hopper feeder was fixed at 50 rpm. Films extruded were collected in a chill roll attachment LabTech Scientific LBCR-150 (Bangkok, Thailand) at 5 m/s.

Ethylene adsorption of active films

The ethylene concentration was quantified using a GC-gas chromatograph as described above. Films of 10 x 5 cm (10g) were placed in a 0.25 L flask and plugged with a rubber cap. The cap was equipped with two pipes, with one being the inlet and the other the outlet for the ethylene gas. The gas sample of 1 mL from the headspace of a 0.25-L flask was injected into the gas chromatograph to determine the ethylene concentration for 10 days. The ethylene adsorption capacity was calculated by subtraction of the initial ethylene concentration from the measured ethylene concentration.

RESULTS AND DISCUSSION

Physicohemical characteristics of the aluminosilicates

The main physicochemical characteristics of the MtNa$^+$ and NZ-Ch are shown in Table 1. Moisture content of the aluminosilicates were 4.40% and 5.16% for MtNa$^+$ and NZ-Ch respectively, values that are in accordance with those reported for commercial montmorillonite (4-9%)[18]. Nevertheless, moisture of NZ-Ch are much higher than value reported for natural zeolite (2.5%)[11]. Specific mass ranged from 2.19 g cm^{-3} to 2.59 g cm^{-3} for MtNa$^+$ and NZ-Ch respectively. These values are also in accordance with those reported for montmorillonite (2.50-2.76 g cm^{-3})[12, 19] and zeolites (2.36-2.39 g cm^{-3})[11,12].

Size distribution analyze

The size distribution analyze showed that 100% of the particles have minor size of 45µm (MtNa$^+$) and a minor size of 75µm for NZ-Ch (Table 1).

Table 1: Main characteristics of the MtNa+ y NZ-Ch.

Characteristics	Mt Na$^+$	NZ-Ch
Moisture (%)	4.40 ± 0.16	5.16 ± 0.09
Specific gravity (g cm^{-3})	2.59 ± 0.23	2.19 ± 0.06
Surface area EGME (m^2 g^{-1})	606.7±14.4	49.80± 0.52
Cation-exchange capacity (meq g^{-1})	1.11 ± 0.08	1.94 ± 0.05

The particle size distribution is related with the kinetics of the ion-exchange[10]. Particle size distribution of MtNa$^+$ and NZ-Ch obtained through the pipette method based on Stoke's law are shown in Table 2. It can be observed that MtNa$^+$ particle diameters are lower than those of the NZ-Ch. This is evidenced by observing that 99% of the particles of MtNa$^+$ have a diameter lower than 20 mm, while in the case of zeolite only 75% of the particles have a diameter under this value. The particle size has an important role in processes of adsorption and desorption, since a smaller particle size means a greater contact surface for adsorbing determined substances. From these values it is expected that MtNa$^+$ present greater ethylene adsorption capacity than NZ-Ch.

Table 2: Particle size distribution.

Particle size (mm)	Mt Na$^+$ (%)	NZ-Ch (%)
$f < 2$	81.46±0.12	20.2±0.05
$2 < f < 20$	18.23±0.89	54.4±1.40
$20 < f < 50$	0.31±1.02	21.9±1.10
$f > 50$	0.00±0.00	3.5±0.30

Specific surface area

Polar liquid retention methods measure the total specific surface area (SSA) of the minerals, although the EGME method can partially measure internal surfaces of soils. In Table 1 it can be observed the differences in SSA values for both aluminosilicates, reaching values of 607 m^2 g^{-1} for MtNa$^+$ and 49.8 m^2 g^{-1} for NZ-Ch. Similar values, 615-815 m^2 g^{-1} have been reported for natural montmorillonite from North Patagonia, Argentina[20] and 25.5-30.1 m^2 g^{-1} for natural New Zealands zeolites (mordenite)[21]. The different structure of MtNa$^+$ (a laminar structure) compared with a porous structure of zeolites justify the differences on the SSA values observed for both minerals.

Cation exchange capacity

The cation exchange capacity (CEC) considers the capacity of the intrinsic ions of the minerals to be exchanged for other species with the same electrical charge. CEC for MtNa$^+$ was 1.11 (meq g^{-1}) meanwhile for NZ-Ch CEC value reached 1.94 (meq g^{-1}). These values are in accordance with those reported for montmorillonite (1.10 meq g^{-1})[16, 22]. Higher CEC values for zeolites have also been reported, with values nearby 2.05 meq g^{-1} [10]. Studies indicate that the generation of negative charge of aluminosilicate minerals is due to the isomorphic substitution between silicon and aluminum atoms. The adsorption properties of gaseous substances depend largely on the exchangeable cations that are much more important for zeolites with a porous structure[23, 24].

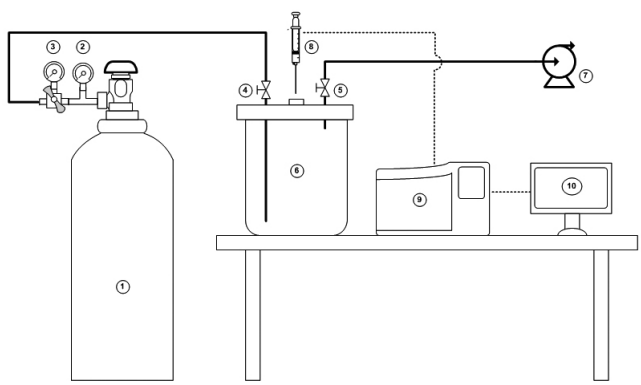

Figure 2: Schematic design of the volumetric adsorption system for films. (1) ethylene cylinder; (2) cylinder manometer; (3) mass flow meters; (4 and 5) valves; (6) adsorption cell; (7) vacuum pump; (8) sampling syringe; (9) gas chromatographic; (10) computer.

Elemental chemical analysis

Chemical composition of $MtNa^+$ and NZ-Ch obtained by elemental chemical analysis are present in Table 3. The main chemical elements for both aluminosilicates, are silicon (71.05%w/w for $MtNa^+$ and 79.05%w/w for NZ-Ch) and aluminum (6.60% w/w for $MtNa^+$ and 4.05%w/w for NZ-Ch). Results of the chemical analysis showed that the natural zeolites contains a complement of exchangeable cations such as Ca^{2+}, K^+, Mg^+, Na^+ and Fe^{3+}. As expected, the main compensating cation present in montmorillonite was sodium (2wt%) because it is a commercial modified montmorillonite (Cloisite Na^+). For NZ-Ch the main compensating cations were calcium, (1.7 wt%), sodium (1.04 wt%) and potassium (0.79 wt%). These cations have importance roles in ion-exchange with other cations in solution such as ammonium[25]. Interestingly, both aluminosilicate presented a low content of copper, however this content was double for NZ-Ch (12.3 mg kg^{-1}) than for $MtNa^+$ (5.5 mg kg^{-1}). The Cu^{2+} cations favors olefin adsorption, they act as active sites of adsorption gas on aluminosilicates[26]

Table 3: Chemical composition of the $MtNa^+$ y NZ-Ch.

Element	Mt Na^+	NZ-Ch
Silicon, % w/w	71.05 ± 3.40	79.05 ± 1.48
Aluminum, % w/w	6.60 ± 0.42	4.05 ± 0.49
Magnesium, % w/w	0.30 ± 0.03	0.13 ± 0.04
Calcium, % w/w	0.39 ± 0.02	1.70 ± 0.14
Iron, % w/w	1.90 ± 0.00	1.15 ± 0.07
Sodium, % w/w	2.00 ± 0.14	1.04 ± 0.08
Potassium, % w/w	0.08 ± 0.01	0.79 ± 0.01
Copper, mg/Kg	4.60 ± 1.27	9.95 ± 3.32

X-ray difracction analysis

Figure 3 shows XRD diffraction patterns of $MtNa^+$ and NZ-Ch. $MtNa^+$ shows the characteristic pattern for Cloisite Na^+, with a basal spacing between the clay layers appeared at 2q=7.49°, corresponding to 1.18 nm[27, 28]. On the other hand, XRD diffraction analysis of natural zeolite showed that the positions and intensities of many of the reflections peaks at 2q=6.58°, 9.84°, 13.54°, 15.40°, 19.74°, 22.34°, 25.78°, 27.78°, 32.04° and 35.78°correspond to the literature data of mordenite[29, 30, 31], as the predominant phase[32].

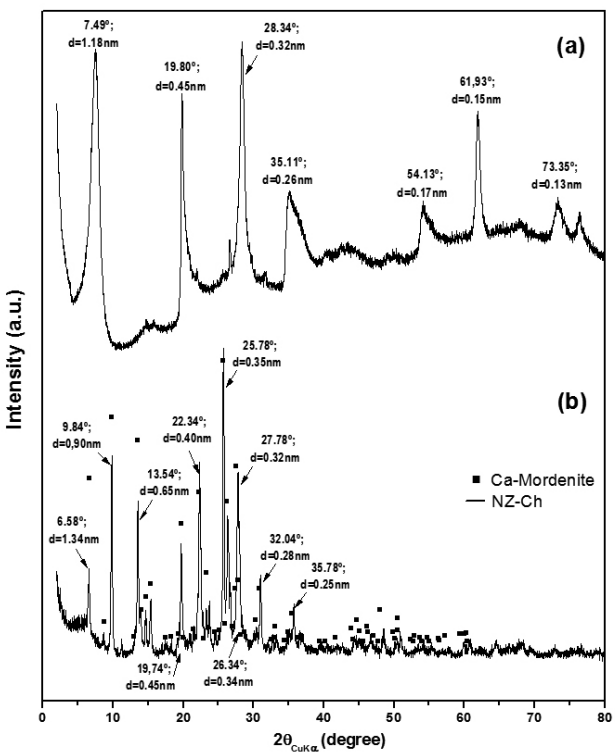

Figure 3: XRD patterns between 2θ=2.00º - 80.00º of (a) $MtNa^+$ and (b) NZ-Ch.

Fourier Transform Infrared Analysis

Figure 4 presents FTIR spectra of $MtNa^+$ and NZ-Ch, that include bands at ~3635 cm^{-1} and ~3437 cm^{-1}, associated with the stretching modes of Si-OH and OH groups of the interlayer water. A band at ~1640cm^{-1} attributed to the –OH bending of absorbed water, and ~1045 cm^{-1} corresponding to Si-O stretching[33, 34, 28]. Other bands characteristic are ~1067, ~796 and ~469. The ~1067 cm^{-1} band corresponds to asymmetric stretching vibration modes of internal T–O bonds in TO_4 tetrahedra (T=Si and Al). The ~796 and ~469 cm^{-1} bands are assigned to the stretching vibration modes of O–T–O groups and the bending vibrations of T-O bonds, respectively[35].

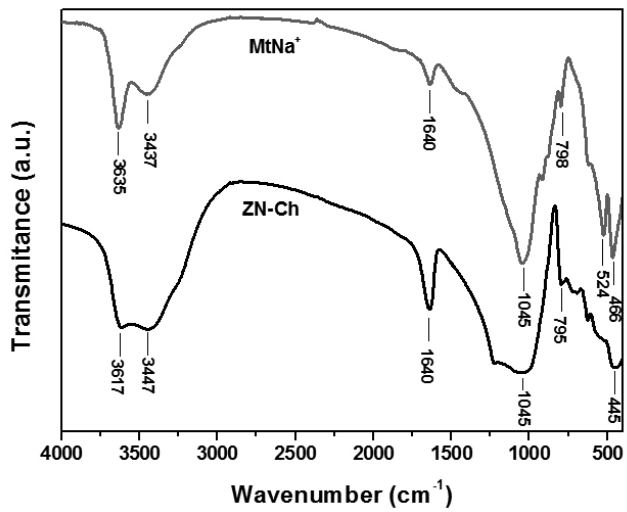

Figure 4: The FTIR spectra of $MtNa^+$ and NZ-Ch.

Ethylene Adsorption

The parameters for pseudo-first and pseudo-second-order kinetic models are listed in Table 4. As it can be seen, although both model well fitted experimental data, the pseudo-second-order model fitted the best with a correlation coefficient of 0.993 for $MtNa^+$ and 0.999 for NZ-Ch. Moreover, the q_e calculated (μL g^{-1}) achieved using the pseudo-second-model is much similar to the q_e experimental (μL g^{-1}), than the obtained with the pseudo-first-order model. Figure 5 shows a plot of pseudo-second-order kinetic model for the ethylene adsorption for $MtNa^+$ and NZ-Ch. For $MtNa^+$ equilibrium is reached after 60 min, meanwhile NZ-Ch reached equilibrium in 30 min. When equilibrium is reached in short periods of time, indicates that the adsorption mechanism is governed by physical interactions, meanwhile long periods of time to reach equilibrium, indicates chemical adsorption or difficulty of accessing the active sites of the adsorbent surface[36]. On the other hand, the value of the rate constant for pseudo-second-order k_2 (g μL^{-1} min^{-1}) is nearly double for NZ-Ch compared with $MtNa^+$. The pore size of zeolite plays an important role on adsorption properties. The larger pore diameter (12Å) reported for a natural zeolite, favour that ethylene (kinetic diameter 3.9 Å) can pass through zeolite pore openings[1], and can be absorbed within the zeolite framework. Two important interactions have been use to describe ethylene adsorption phenomena, first a cation-p interaction which occurs between p–electrons of double bond of ethylene and metal cations, which involves s-donation and p* back donation between the metal cations and de *p* orbital of ethylene, and also a CH-O interaction, a weak hydrogen bonding between hydrogen atoms of ethylene and oxygen atoms at the zeolite surface, which is weakly electropositive[2, 4].

Table 4: Adsorption kinetics parameters on $MtNa^+$y NZ-Ch.

Sample	$q_{e,exp.}$ (μL g^{-1})	Pseudo-first-order model			Pseudo-second-order model		
		$q_{e,cal.}$ (μL g^{-1})	K_1 (min^{-1})	R^2	$q_{e,cal.}$ (μL g^{-1})	K_2 (g μL^{-1} min^{-1})	R^2
$MtNa^+$	0.155	0.1472	0.0435	0.988	0.1575	0.7084	0.993
NZ-Ch	0.885	0.8698	0.2015	0.987	0.8868	1.3375	0.999

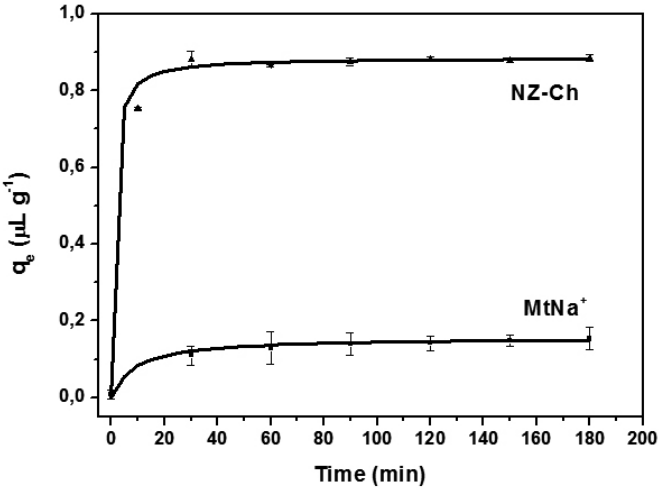

Figure 5: Ethylene adsorption kinetics on $MtNa^+$ y NZ-Ch. Co= 9.6 ppm ; T=25ºC ; P=1atm.

Adsorption isotherms

Adsorption isotherm is one of the most important parameters to find the adsorption mechanism. Langmuir isotherm model can be applied for the determination of the maximum monolayer adsorption capacity of the adsorbent. The ethylene gas adsorption isotherms, expressed as absolute amount of ethylene adsorbed per gram of adsorbent are shown in Figure 6. The curves are similar in shape, and have classic isotherm type I form[1]. The values of the constants in the models and the correlation coefficients obtained are summarized in Table 5. The applicability of Langmuir-Freundlich isotherm suggests a monolayer coating of ethylene molecules onto aluminosilicates surface. From the Langmuir-Freundlich parameters the maximum adsorption of ethylene capacity (q_m) were calculated, being 1.28 µl g^{-1} for $MtNa^+$ y 5.42 µl g^{-1} for NZ-Ch, which shows clearly that the NZ-Ch presents higher adsorption capacity compared with $MtNa^+$, indicating a high affinity between the adsorbent and the adsorbate. This result was not expected due to the physicochemical properties initially reported, where $MtNa^+$ presented a smaller particle size and higher specific surface area. Nevertheless, the porous structure of zeolites favours the adsorption mechanism, and on the other hand zeolite presented higher amount of copper and calcium, and divalent cations in zeolites are known to be strong adsorptive center[1]. It has been reported chabazite-type zeolite to remove 94% of ethylene incorporated in a jar with 48% relative humidity[37], values similar to those reported for commercial potassium permanganate with a removal capacity of 91% of the ethylene present in a apple packaging system[38].

Table 5: Adsorption isotherm parameters on $MtNa^+$y NZ-Ch.

Muestra	Langmuir-Freundlich model			
	q_m (µl g^{-1})	b (ppm^{-1})	n	R^2
$MtNa^+$	1.28034	5.61E-44	0.0207	0.9985
NZ-Ch	5.41882	0.7841	0.7166	0.9982

Between both aluminosilicate it is reasonable to select NZ-Ch as a mineral in which its intrinsic ethylene adsorption capacity could be improved in order to design a new ethylene scavenger to develop a new food packaging system oriented to increase the shelf-life of climacteric fruits.

Ethylene Adsorption on films

Figure 7 shows the ethylene adsorption kinetics of LDPE films with different NZ-Ch contents (0, 2.5, 5, 7.5, 10 % w/w). It can be observed than LDPE film already presented a slight ethylene removal capacity, producing a decrease of the ethylene concentration in the headspace of 8% aproximately. On the other hand for the rest of the films, in the first 50 hours a fast reduction of the ethylene concentration can be observed, meanwhile after 50 hours the rate of the ethylene removal is much slower. The presence of NZ-Ch produces a decrease on the ethylene concentration in the headspace in accordance with the content of active mineral, reaching a decrease of 37% of the ethylene content for films containing 10% of ZN-Ch after 100 h.

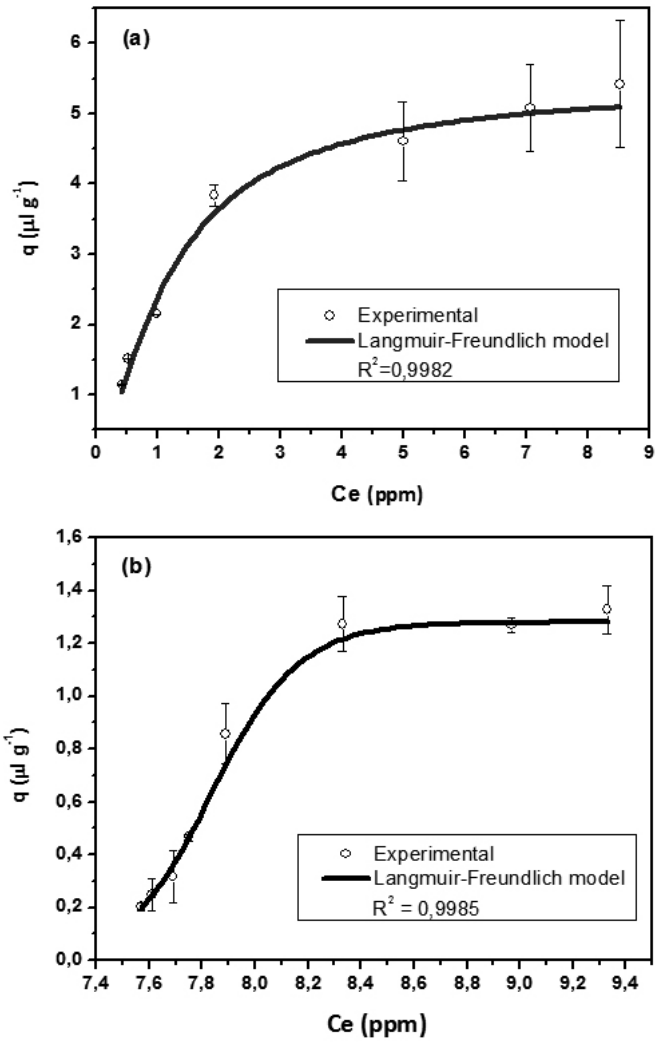

Figure 6: Adsorption isotherm at 25ºC; (a) $MtNa^+$ and (b) NZ-Ch.

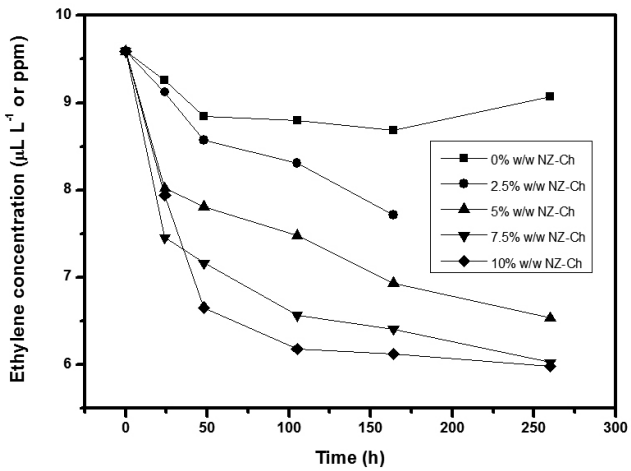

Figure 7: Ethylene adsorption on film of natural zeolite and LDPE. Co= 9.6 ppm ; T=25ºC; P=1atm.

CONCLUSIONS

In this study, the efficiency of a Chilean natural zeolite (NZ-Ch) against a commercial Na^+ montmorillonite (Cloisite Na^+) was studied. The aluminosilicate characterization demostrated that natural Chilean zeolite belongs to mordenite group, and it presents a specific surface area of 607 m^2g^{-1}, much higher that the specific surface area of CloisiteNa^+ (49.8 m^2g^{-1}). Elemental chemical analysis indicated that as expected silicon and aluminium were the main elements of the both aluminosilicate, being the compensating ions, sodium for MTNa^+ and calcium, sodium and potassium for NZ-Ch. In both cases copper was present in their composition.

Ethylene adsorption kinetics were fitted to a pseudo-second order model. The rate constant of the ethylene adsorption was nearly double for NZ-Ch compared with MtNa^+. Langmuir-Freundlich isotherm allowed to determine maximum adsorption capacity that reached values of 5.4 for NZ-Ch and 1.28 for CloisiteNa^+.

Higher ethylene capacity of NZ-Ch was attributed to their porous structure and to the presence of copper as compensating cation, as it enhances adsorption properties of aluminosilicate, as act as a active site of adsorption.

ACKNOWLEDGEMENTS

The authors thanks to Fondo de Fomento al Desarrollo Científico y Tecnológico (Project FONDEF D11I1123) and Programa de Financiamiento Basal para Centros Científicos y Tecnológicos de Excelencia (Project FB0807). Alejandro Coloma thanks to Comisión Nacional de Investigación Científica y Tecnológica, CONICYT, for giving the National Doctoral Scholarship for Foreign Students.

REFERENCES

1. B. Erdoğan, M. Sakızcı, E. Yörükoğulları, *Applied Surface Science* **254**, 2450, (2008).
2. N. Patdhanagul, T. Srithanratana, K. Rangsriwatananon, S. Hengrasmee, *Microporous and Mesoporous Materials* **131**, 97, (2010).
3. L. A. Terry, T. Ilkenhans, S. Poulston, L. Rowsell, A. W. J. Smith, *Postharvest Biology and Technology* **45**, 214, (2007).
4. N. Patdhanagul, K. Rangsriwatananon, K. Siriwong, S. Hengrasmee, *Microporous and Mesoporous Materials* **153**, 30, (2012).
5. V. K. Saini, M. Pinto, J. Pires, *Separation Science and Technology* **46**, 137, (2011).
6. C. A. Ríos, L. Y. Vargas, in *Earth and Environmental Sciences,* I. A. Dar, M. A. Dar, Eds. InTech, Rijeka, 2011, pp. 363-374.
7. S. Navalon, M. Alvaro, H. Garcia, *Applied Catalysis B: Environmental* **99**, 1, (2010).
8. N. Sue-aok, T. Srithanratana, K. Rangsriwatananon, S. Hengrasmee, *Applied Surface Science* **256**, 3997, (2010).
9. B. Erdoğan, M. Sakizci, *Adsorption Science & Technology* **30**, 265, (2012).
10. A. H. Englert, J. Rubio, *Int. J. Miner. Process* **75**, 21, (2005).
11. C. d. R. Oliveira, J. Rubio, *Materials Research* **10**, 407, (2007).
12. Y. Yukselen, A. Kaya, *Journal of Geotechnical and Geoenvironmental Engineering* **132**, 931, (2006).
13. G. Montenegro, C. Fredes, E. Mejías, C. Bonomelli, L. Olivares, *Agrociencia* **43**, 427, (2009).
14. B. L. R. Braga, C. I. G. L. Sarantópoulos, L. Peres, J. W. B. Braga, *Packag. Technol. Sci.* **23**, 351, (2010).
15. M. J. Galotto, S. A. Anfossi, A. Guarda, *Food Sci Tech Int* **15**, 159, (2009).
16. H. Nourmoradi, M. Khiadani, M. Nikaeen, *Journal of Chemistry* **2013**, 1, (2013).
17. S. Hosseinpour, S. Fatemi, Y. Mortazavi, M. Gholamhoseini, M. T. Ravanchi, *Separation Science and Technology* **46**, 349, (2011).
18. R. Zahedsheijani, H. Gholamiyan, A. Tarmian, H. Yousefi, *Maderas. Ciencia y tecnología* **13**, 163, (2011).
19. S. I. S. Shahabadi, H. Garmabi, *eXPRESS Polymer Letters* **6**, 657, (2012).
20. B. Lombardi, M. Baschini, R. M. Torres Sánchez, *The Journal of the Argentina Chemical Society* **90**, 87, (2002).
21. M. L. Nguyen, C. C. Tanner, *New Zealand Journal of Agricultural Research* **41**, 427, (1998).
22. C. Volzone, J. G. Thompson, A. Melnitchenko, J. Ortiga, S. R. Palethorpe, *Clays and Clay Minerals* **47**, 647, (1999).
23. G. Aguilar-Armenta *et al.*, *J. Phys. Chem. B* **105,** 1313, (2001).
24. D. L. Carter, M. M. Mortland, W. D. Kemper, in *Methods of Soil Analysis: Physical and mineralogical methods, Part I,* A. Klute, A. L. Page, Eds. American Society of Agronomy, Michigan, 1986, vol. 9, pp. 413-423.
25. N. Widiastuti, H. Wu, H. M. Ang, D. Zhang, *Desalination* **277**, 15 (2011).
26. A. N. Il'ichev, V. A. Matyshak, V. N. Korchak, Y. B. Yan, *Kinetics and Catalysis.* **42**, 706 (2000).
27. J. E. Bruna, A. Peñaloza, A. Guarda, F. Rodríguez, M. J. Galotto, *Applied Clay Science* **58**, 79, (2012).
28. F. J. Rodriguez, M. J. Galotto, A. Guarda, J. E. Bruna, *Journal of Food Engineering* **110**, 262, (2012).
29. T. Nakamura, M. Ishikawa, T. Hiraiwa, J. Sato, *Analytical Sciences* **8**, 539, (1992).
30. S. Sohrabnezhad, A. Rezaei, *Superlattices and Microstructures* **55**, 168, (2013).
31. M. M. J. Treacy, J. B. Higgins, *Collection of Simulated XRD Powder Patterns for Zeolites*. Stucture Commision of the International Zeolite Association, USA, ed. Fourth, 2001.
32. C. Covarrubias, R. García, R. Arriagada, J. Yánez, M. T. Garland, *Microporous and Mesoporous Mater.* **88**, 220, (2006).
33. H. A. Patel, R. S. Somani, H. C. Bajaj, R. V. Jasra, *Applied Clay Science* **35**, 194, (2007).
34. A. R. Ramadan, A. M. K. Esawi, A. A. Gawad, *Applied Clay Science* **47**, 196, (2010).
35. N. Mansouri, N. Rikhtegar, H. A. Panahi, F. Atabi, B. K. Shahraki, *Environmental Protection Engineering* **39**, 139, (2013).
36. S. R. Taffarel, J. Rubio, *Minerals Engineering* **23**, 771, (2010).
37. G. Peiser, T. V. Suslow, *Perishables Handling Quarterly* **17**, 1, (1998).
38. R. B. H. Wills, M. A. Warton, *J. Amer. Soc. Hort. Sci.* **129**, 433, (2004)**.**